

RESEARCH ARTICLE

Open Access



A potential cost of evolving epibatidine resistance in poison frogs

Julia M. York^{1,2}, Cecilia M. Borghese¹, Andrew A. George^{3,4†}, David C. Cannatella^{2†} and Harold H. Zakon^{1,2*†} 

Abstract

Background Some dendrobatid poison frogs sequester the toxin epibatidine as a defense against predators. We previously identified an amino acid substitution (S108C) at a highly conserved site in a nicotinic acetylcholine receptor β 2 subunit of dendrobatid frogs that decreases sensitivity to epibatidine in the brain-expressing α 4 β 2 receptor. Introduction of S108C to the orthologous high-sensitivity human receptor similarly decreased sensitivity to epibatidine but also decreased sensitivity to acetylcholine, a potential cost if this were to occur in dendrobatids. This decrease in the acetylcholine sensitivity manifested as a biphasic acetylcholine concentration–response curve consistent with the addition of low-sensitivity receptors. Surprisingly, the addition of the β 2 S108C into the α 4 β 2 receptor of the dendrobatid *Epipedobates anthonyi* did not change acetylcholine sensitivity, appearing cost-free. We proposed that toxin-bearing dendrobatids may have additional amino acid substitutions protecting their receptors from alterations in acetylcholine sensitivity. To test this, in the current study, we compared the dendrobatid receptor to its homologs from two non-dendrobatid frogs.

Results The introduction of S108C into the α 4 β 2 receptors of two non-dendrobatid frogs also does not affect acetylcholine sensitivity suggesting no additional dendrobatid-specific substitutions. However, S108C decreased the magnitude of neurotransmitter-induced currents in *Epipedobates* and the non-dendrobatid frogs. We confirmed that decreased current resulted from fewer receptors in the plasma membrane in *Epipedobates* using radiolabeled antibodies against the receptors. To test whether S108C alteration of acetylcholine sensitivity in the human receptor was due to (1) adding low-sensitivity binding sites by changing stoichiometry or (2) converting existing high- to low-sensitivity binding sites with no stoichiometric alteration, we made concatenated α 4 β 2 receptors in stoichiometry with only high-sensitivity sites. S108C substitutions decreased maximal current and number of immunolabeled receptors but no longer altered acetylcholine sensitivity.

Conclusions The most parsimonious explanation of our current and previous work is that the S108C substitution renders the β 2 subunit less efficient in assembling/trafficking, thereby decreasing the number of receptors in the plasma membrane. Thus, while β 2 S108C protects dendrobatids against sequestered epibatidine, it incurs a potential physiological cost of disrupted α 4 β 2 receptor function.

Keywords Evolution, Nicotinic acetylcholine receptor, Poison frog, Epibatidine, *Epipedobates anthonyi*, *Xenopus tropicalis*, *Nanorana parkeri*

[†]Andrew A. George, David C. Cannatella, and Harold H. Zakon contributed equally as senior authors.

*Correspondence:

Harold H. Zakon

h.zakon@austin.utexas.edu

Full list of author information is available at the end of the article



Background

Some animals sequester alkaloid toxins for defense. Many of these alkaloids target ion channels, ion pumps, or neurotransmitter receptors [1, 2]. Because the sequestered alkaloids are present within their tissues, defended animals (or their predators) must evolve protection from these toxins. This frequently occurs by adaptive amino acid substitutions at the target molecule [1–3], which may come with a cost of decreased function of that molecule [4–6] and decreased organismal performance. Because there may be a tradeoff between successful defense against predators and fitness [7], an important step in understanding the adaptive value of a sequestered toxin is a determination of the proximate cost of evolving target resistance.

Numerous neotropical poison frog species derive alkaloids from their arthropod prey, typically ants and mites, and sequester these toxins for defense [8–10]. For example, at least three genera sequester alkaloid agonists or antagonists for nicotinic acetylcholine receptors (nAChRs) which, in turn, disrupts acetylcholine-based synaptic transmission. Frogs, like mammals, have numerous cholinergic neurons in their brains [11, 12], and some species have evolved resistance to their dietary alkaloids. In particular, species of *Epipedobates* poison frogs sequester the alkaloid epibatidine, well-studied for its agonist action on nAChRs that contain $\beta 2$ subunits, and we previously demonstrated epibatidine-resistance in at least one brain-expressed isoform of the nAChR [13].

nAChRs exist as a diverse family of molecules composed of different pentameric combinations of homologous subunits derived from at least 17 genes ($\alpha 1$ – $\alpha 10$, $\beta 1$ – $\beta 4$, γ , δ , ϵ). The properties of nAChRs are determined by their subunit composition, giving rise to multiple subtypes with a range of overlapping pharmacological and biophysical properties [14]. In mammals, the major brain isoform of the nAChR is composed of $\alpha 4$ and $\beta 2$ subunits which appears in two alternate stoichiometries [15] (Additional file 1). Two $\alpha 4$ and three $\beta 2$ subunits ($2\alpha:3\beta$) produce an isoform of the receptor with high sensitivity (HS) to ACh where ACh binds at $\alpha(+):\beta(-)$ interfaces (Additional file 1, panel A). A low-sensitivity (LS) binding site is also naturally present when the receptors within the central nervous system express three $\alpha 4$ and two $\beta 2$ subunits ($3\alpha:2\beta$, Additional file 1, panel B). LS sites, which occur at the interface between two adjacent $\alpha 4$ subunits [i.e., $\alpha(+):\alpha(-)$] [16, 17], can influence the function of the pentameric $\alpha 4\beta 2$ nAChR by providing an additional low-affinity binding site for ACh [18, 19].

Experimental expression of nAChRs in *Xenopus* oocytes has been critical for understanding their normal function [20, 21], pathology [22–24], and pharmacology, including responses to epibatidine [25, 26], because

many of their properties (as measured in vivo) can be replicated in this heterologous system. Pertinent to this study, the naturally occurring differences in ACh sensitivity can be replicated in *Xenopus* oocytes by varying the RNA ratio of $\alpha 4$ and $\beta 2$ subunits [27, 28]. An abundance of $\alpha 4$ RNA favors $3\alpha:2\beta$ with both HS- and LS-binding sites, whereas an abundance of $\beta 2$ RNA favors $2\alpha:3\beta$ with only HS-binding sites (Additional file 2, panels A and B). This observation has been verified with concatemers with fixed ratios of $\alpha 4$ and $\beta 2$ subunits [29].

In our previous work, we noted a serine to cysteine substitution (S108C) that evolved independently in the $\beta 2$ nAChR subunit in three genera of dendrobatid frogs (*Epipedobates*, *Ameerega*, *Oophaga*) that possess alkaloids which target $\alpha 4\beta 2$ nAChRs [13] (Fig. 1). The serine at this site is highly conserved across vertebrate $\beta 2$ nAChR subunits over 550 million years of evolutionary time (Fig. 1 and Additional file 3) [30]. We assume that S108 is the ancestral residue for the three genera of dendrobatid frogs based upon a parsimony argument: its universal presence in vertebrate $\beta 2$ subunits and the fact that a single nucleotide change is sufficient to effect a serine to cysteine substitution makes it unlikely that any other amino acid would have occurred in the ancestors of each lineage. We found that introduction of the S108C substitution into the human $\alpha 4\beta 2$ nAChR ($1\alpha:3\beta$ RNA ratio expressed in *Xenopus* oocytes, which should produce only HS sites) conferred epibatidine resistance [13] but also produced LS sites, reducing the sensitivity to ACh as detected in concentration–response curves (CRCs) (Additional file 2, panel A). At a $3\alpha:1\beta$ RNA ratio, the introduction of S108C added even more LS sites, further reducing the sensitivity to ACh by shifting the ACh CRC rightward (Additional file 2, panel B). We also noted substitutions at other highly conserved sites near S108C in other dendrobatids (*Epipedobates* and *Ameerega*) (Fig. 1). Introduction of F106L, a novel phenylalanine to leucine substitution in *Epipedobates*, into the human $\beta 2$ nAChR subunit with the S108C substitution partially (3:1) or completely (1:3) restored baseline ACh sensitivity (i.e., LS sites were eliminated) (Additional file 2, panels A and B). Therefore, the novel presence of both L and C decreases sensitivity to epibatidine in human $\alpha 4\beta 2$ nAChRs while maintaining a normal response to ACh, which would presumably be advantageous for frogs defended by epibatidine.

Having tested the response in human $\alpha 4\beta 2$ nAChRs, we predicted that the wild-type *Epipedobates* receptor, which evolved the S108C and F106L substitutions, would likewise possess resistance to epibatidine and incur a similar decrease in ACh sensitivity (due to the C108), but this decreased ACh sensitivity would be rescued by its second substitution (leucine instead of the

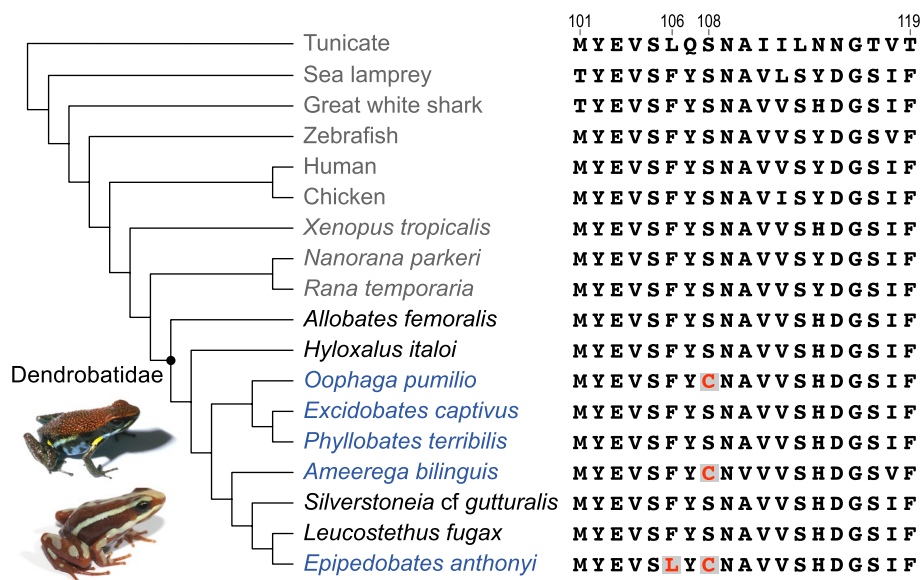


Fig. 1 Phylogeny of selected chordates showing the variation of amino acid sequences in the region of interest of the β_2 nAChR subunit. Scientific names are used for the frogs. The dot in the phylogeny represents the ancestor of the poison frogs (Dendrobatidae clade). The names of undefended species of poison frogs are in black, and those of defended species are in blue. Defense by sequestered alkaloids appears to have evolved three times, associated with the parallel evolution of S108C and the unique evolution of F106L in *Epipedobates*. Accession numbers and names of the species included in this figure can be found in Additional file 3. Photos of *Ameerega bilinguis* and *Epipedobates anthonyi* (from which epibatidine was first isolated) are shown in the lower left. Photos courtesy of David Cannatella

ancestral phenylalanine) [13]. However, while the *Epipedobates* wild-type $\alpha_4\beta_2$ nAChR (expressed after injection of either 1:7 or 7:1 $\alpha_4:\beta_2$ RNA ratio) showed epibatidine resistance [13], there was surprisingly little decrease in the ACh sensitivity between the two ratios (i.e., no LS sites) (Additional file 2, panels D and E), even when RNA was injected in a ratio that strongly favors the formation of LS sites in mammalian nAChRs (7 α :1 β) (Additional file 2, panel E). Reverting C108 to the ancestral serine (S) eliminated epibatidine resistance but did not decrease ACh sensitivity (in either 1:7 or 7:1 $\alpha_4:\beta_2$ RNA ratios). Additionally, reverting the leucine at position 106 to the ancestral phenylalanine had no effect either on the ACh (Additional file 2, panels D and E) or the epibatidine CRCs observed in *Epipedobates* $\alpha_4\beta_2$ nAChRs [13]. The data from the *Epipedobates* $\alpha_4\beta_2$ receptor appeared to contradict our initial hypothesis that the cost of epibatidine resistance for poison frogs is decreased ACh sensitivity. However, that prediction was based on data from the human receptor in which α_4 and β_2 subunits were free to oligomerize in one of two stoichiometries. Therefore, it was imperative to test functional changes induced when a Cys substituted β_2 Ser108 in the $\alpha_4\beta_2$ receptor of non-dendrobatid frogs compared to those of humans, and also from those of *Epipedobates*. If the receptors from *Epipedobates* differ from other frogs, it would support the hypothesis of dendrobatid-specific substitutions that

protect ACh sensitivity. Furthermore, in our previous work, it was not clear whether the change in ACh sensitivity conferred by S108C was due to the addition of LS sites by a change in subunit stoichiometry or the conversion of existing HS sites to LS sites with no stoichiometric alteration. We, therefore, wished to assess whether S108C perturbs ACh sensitivity in the human $\alpha_4\beta_2$ receptor by the addition of LS sites in a concatenated receptor with a fixed stoichiometry that would normally produce only HS sites.

Here, by examining ACh sensitivity in two non-dendrobatid frogs and a concatenated human $\alpha_4\beta_2$ receptor, we test three alternative hypotheses for the unexpected inability of the C108S substitution to alter the ACh sensitivity of the *Epipedobates* nAChR: (1) if the non-dendrobatid receptors show decreased sensitivity to ACh when the S108C substitution is introduced, then other unidentified dendrobatid-specific amino acid substitutions protect the *Epipedobates* receptor; (2) the cost of substituting S108, a highly conserved residue, manifests as a different aspect of receptor function; or (3) this substitution is cost-free. In comparing the neurotransmitter-elicited responses of $\alpha_4\beta_2$ nAChRs from *Epipedobates*, non-dendrobatid frogs, and humans, we found no support for additional dendrobatid-specific substitutions (rejection of hypothesis 1) but observed instead that S108C presents a different potential cost (rejection of hypothesis

3): it decreases the number of $\alpha 4\beta 2$ -containing nAChRs in the plasma membrane (failure to reject hypothesis 2), which could potentially disrupt cholinergic synaptic transmission, presumably leading to a decrease in fitness. Additionally, we determined that the decrease in ACh sensitivity in human receptors when the substitution S108C is introduced was due to the formation of LS-binding sites through a shift to the LS stoichiometry.

Results

The S108C substitution does not affect acetylcholine sensitivity in non-dendrobatid frogs

We tested the “unidentified dendrobatid-specific substitution” hypothesis by examining the effect of the S108C substitution on the ACh sensitivity of the $\alpha 4\beta 2$ nAChR of two deeply divergent [31] species of non-dendrobatid frogs—Western clawed frogs (*Xenopus tropicalis*, 182 million years ago, mya) and high Himalaya frogs (*Nanorana parkeri*, 130 mya)—with the expectation that their receptors would behave more like human receptors than those of dendrobatids.

The ACh CRC from *Xenopus* $\alpha 4\beta 2$ nAChRs was best fit by a monophasic curve with a single EC_{50} (concentration of transmitter that elicits 50% of the maximum response), whether ratios favored (1:3) or disfavored (7:1) the incorporation of $\beta 2$ subunits. The monophasic curve implies a single population of HS receptors with only HS binding sites (Fig. 2A–C; Table 1; Additional file 4). Representative tracings are shown in Additional file 5, panel A and B. LS sites were never observed with either ratio, unlike homologous mammalian receptors that we previously tested (Additional file 2, panel B). We did not detect differences in the ACh CRCs between the *Xenopus* wild-type [with phenylalanine in position 106 and serine in position 108 in the $\beta 2$ subunit, represented with $\beta 2$ (FS)], the S108C-substituted [$\beta 2$ (FC), with bold indicating the substituted residue], or the combined F106L/S108C-substituted nAChRs [$\beta 2$ (LC)]. Interestingly, the *Xenopus* $\alpha 4\beta 2$ nAChR was $\sim 28\times$ more sensitive to ACh than the human receptors (Tables 1 and 3 [13]) and $\sim 9\times$ more sensitive than the *Epipedobates* receptors [13]. This was true even when human and *Xenopus* receptors were tested in the same recording session with the same reagents.

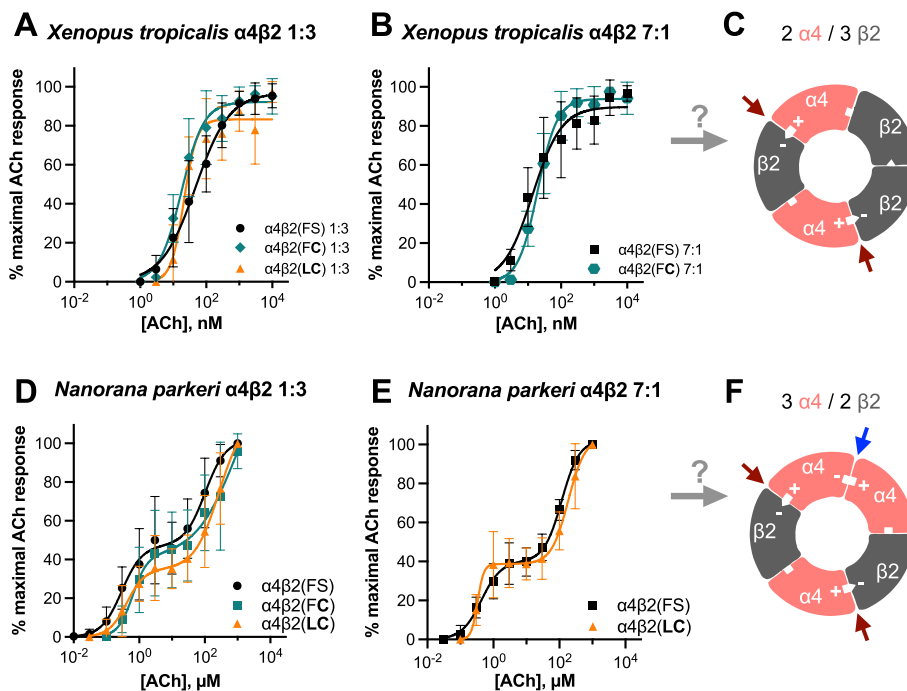


Fig. 2 Acetylcholine CRCs of receptors from two non-dendrobatid frogs. *Xenopus tropicalis* retain a monophasic ACh CRC best fit with a single EC_{50} (Table 1 and Additional file 4) even in conditions that induce LS sites in mammalian $\alpha 4\beta 2$ nAChRs (7 α :1 β) or with the S108C substitution alone [$\beta 2$ (FC)] or in combination with F106L [$\beta 2$ (LC)]. The α : β RNA ratios are 1:3 (A, $n = 6-18$) and 7:1 (B, $n = 13-37$). The actual stoichiometry of frog receptors is unknown but the *Xenopus* $\alpha 4\beta 2$ nAChR behaves as the mammalian 2 α :3 β stoichiometry (C). This conjecture is indicated as a question mark over the gray arrow. Note that the scale for *Xenopus* is nanomolar concentration. *Nanorana parkeri* retain a biphasic CRC best fit with two EC_{50} values (Table 2 and Additional file 4) in both 1:3 (D, $n = 5-9$) or 7:1 (E, $n = 6-9$) α : β RNA ratios, with the S108C substitution alone [$\beta 2$ (FC)] or in combination with F106L [$\beta 2$ (LC)]. The *Nanorana* $\alpha 4\beta 2$ nAChR behaves as if its stoichiometry is 3 α :2 β (F) with both ratios of RNA used in this study. Data points represent means \pm SD. Red arrows indicate HS-binding sites, and blue arrow indicates LS-binding site. + and - signs indicate the principal and complementary components of the subunit interfaces

Table 1 Parameters from a non-linear curve fit of ACh concentration–response curves in oocytes expressing *Xenopus tropicalis* α4β2 nAChRs

cRNA ratio	Receptor	EC ₅₀ (nM)	n _H	I _{max} (%)	n
1:3	α4β2(FS)	47 (37 to 61)	0.85 ± 0.06	97 ± 2	18
	α4β2(FC)	18 (13 to 26)	1.3 ± 0.2	92 ± 3	14
	α4β2(LC)	21 (12 to 43)	2.2 ± 0.8	83 ± 4	6
7:1	α4β2(FS)	14 (8 to 30)	1.0 ± 0.2	90 ± 4	13
	α4β2(FC)	20 (17 to 24)	1.5 ± 0.1	94 ± 1	10
	α4β2(LC)	–	–	–	37

The data from all curves fitted a one-population (monophasic) curve. β2(FS) represents F106 and S108 in the β2 subunit. When used for residues, the bold font indicates substitutions in the wild-type background

Dashes signify currents too small to determine concentration–response curves

EC₅₀ effective concentration 50 (concentration that produces 50% of maximal response), expressed as mean (95% confidence intervals); n_H Hill coefficient, expressed as mean ± SEM; I_{max} maximal current, expressed as a percentage of maximal response (mean ± SEM); n number of oocytes

In contrast, the ACh CRCs of *Nanorana* were biphasic in both 1α:3β and 7α:1β ratios (Fig. 2D, E; Table 2; Additional file 4), implying that each *Nanorana* α4β2 nAChR possesses both HS [α(+):β(–)] and LS [α(+):α(–)] sites in a single, fixed stoichiometry (Fig. 2F), based on a 3α:2β configuration as may occur in mammals. Representative tracings are shown in Additional file 5, panels C and D.

These data demonstrate that the cysteine substitution (S108C) alone or in combination with F106L does not affect ACh sensitivity in non-dendrobatid frogs, leading us to reject the hypothesis that dendrobatid-specific substitutions in the α4β2 nAChR protect against perturbation to CRCs by preventing the ratio-dependent emergence of LS sites as occurs in mammalian receptors. Furthermore, they suggest that, unlike mammalian α4β2 nAChRs, the frog α4β2 nAChRs that we studied have fixed stoichiometries of α and β subunits that cannot be

altered by skewing the ratio of their RNAs, at least in the oocyte expression system and with the ratios of RNAs that we used (Fig. 2C, F). Finally, they show that frogs have surprising species-specific diversity in the ACh CRCs of their α4β2 nAChRs.

S108C substitution reduces peak current amplitudes of expressed frog α4β2 nAChRs

Our second hypothesis is that S108C might perturb a different aspect of receptor function than ACh sensitivity. While measuring CRCs, we noted that the peak current amplitudes (which we call simply “currents” hereafter) from *Xenopus* or *Nanorana* α4β2 nAChRs with the S108C substitution, especially in the 7α:1β ratio, were absent or too miniscule to reliably measure using amounts of RNA that generated substantial currents in wild-type channels. Therefore, especially at ratios of 7α:1β, we increased the total amount of RNA to enhance the currents (Additional file 6). The observation that cysteine-bearing receptors had smaller currents than wild-type receptors, even when higher amounts of RNA were injected, suggested that the presence of cysteine reduces the α4β2 nAChR currents. For example, in *Nanorana*, at 1:3 or 7:1 α4:β2 RNA ratios, S108C with or without F106L reduced currents in both ratios (Additional file 6, panel B).

In our previous study on *Epipedobates* [13], we varied the amount of RNA injected or the number of days of incubation to optimize the current magnitude since our goal was to measure normalized CRCs, which do not vary with the amount of RNA injected or days of incubation. Consequently, we could not directly compare maximal currents within or across experiments. In the current study, in order to make statistically valid comparisons across different amino acid substitutions, we replicated the experiments on *Epipedobates* receptors holding the amount of RNA constant within each condition (α:β

Table 2 Parameters from a non-linear curve fit of ACh concentration–response curves in oocytes expressing *Nanorana* α4β2 nAChRs

cRNA ratio	Receptor	EC _{50_HS} (μM)	EC _{50_LS} (μM)	n _{H_HS}	n _{H_LS}	I _{max_HS} (%)	I _{max_LS} (%)	n
1:3	α4β2(FS)	0.29 (0.18 to 0.49)	102 (63 to 231)	1.4 ± 0.3	1.4 ± 0.4	47.1 ± 3.3	54.7 ± 6.3	9
	α4β2(FC)	0.63 (0.30 to 1.40)	935 (92 to ?)	2.0 ± 0.7	0.7 ± 0.6	41.1 ± 9.7	107 ± 150	5
	α4β2(LC)	0.41 (0.32 to 0.55)	269 (201 to 530)	1.6 ± 0.2	1.2 ± 0.1	35.0 ± 1.4	79.1 ± 6.5	8
7:1	α4β2(FS)	0.43 (0.29 to 0.64)	117 (92 to 151)	1.5 ± 0.2	1.6 ± 0.2	40.0 ± 1.8	62.2 ± 3.5	6
	α4β2(FC)	–	–	–	–	–	–	16
	α4β2(LC)	0.33 (? to 0.35)	184 (173 to 196)	4.6 ± 1.3	1.7 ± 0.1	38.7 ± 0.2	64.8 ± 0.7	9

The data was best fitted by a two-population (biphasic) curve. β2(FS) represents F106 and S108 in the β2 subunit. When used for residues, the bold font indicates substitutions in the wild-type background

The two components of the biphasic curve are characterized by different parameters. HS stands for high sensitivity, and LS for low sensitivity. Dashes signify currents too small to determine concentration–response curves. Sometimes, the statistical analysis software is unable to determine one of the confidence limits, represented by a question mark

EC₅₀ effective concentration 50 (concentration that produces 50% of maximal response), expressed as mean (95% confidence intervals); n_H Hill coefficient, expressed as mean ± SEM; I_{max} maximal current, expressed as a percentage of maximal response (mean ± SEM); n number of oocytes

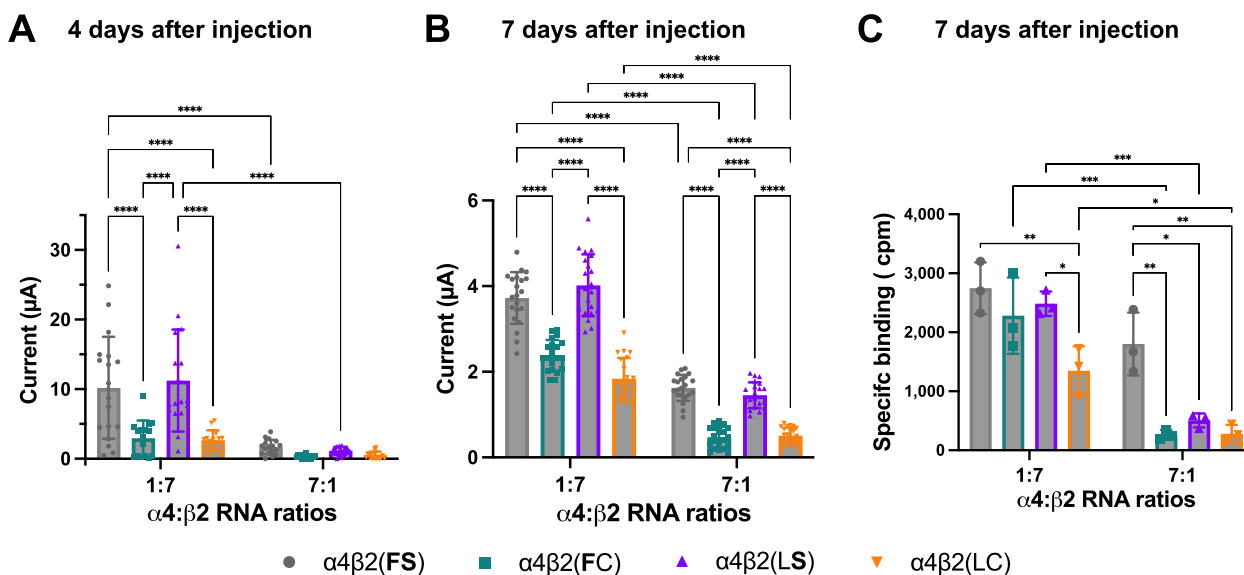


Fig. 3 Maximal ACh-induced current and labeling of *Epipedobates anthonyi* $\alpha 4\beta 2$ nAChRs. Maximal ACh-induced currents were measured at 4 (**A**, $n = 14\text{--}18$ oocytes) and at 7 (**B**, $n = 21$) days after injection. The presence of cysteine in location 108, either combined with F106 [$\beta 2$ (FC), green] or with L106 [$\beta 2$ (LC), wild type, orange], decreases the magnitude of ACh-stimulated maximal currents through the $\alpha 4\beta 2$ receptors, compared with $\beta 2$ (FS) (gray) and $\beta 2$ (LS) (violet). The bold font indicates a substitution introduced in the wild-type receptor. Following recordings shown in **B**, oocytes were treated with the radiolabeled antibody ^{125}I -mAb 295 to quantify the specific binding, i.e., the number of $\beta 2$ -containing nAChRs expressed in the plasma membrane (**C**, $n = 3, 7$ pooled oocytes each experiment). Cpm stands for counts per minute. $\alpha 4\beta 2$ RNA injection ratios favoring HS (1:7) and LS (7:1) stoichiometries are indicated on the X-axis. Data are presented as means \pm SD and were analyzed using two-way ANOVA, followed by pairwise comparisons corrected for multiple comparisons with Holm-Sidak's test. * $P < 0.05$, ** $P < 0.01$, *** $P < 0.001$, **** $P < 0.0001$

ratio) and incubating oocytes for 4 or 7 days in two independent replicates. In both replicates, we observed in the *Epipedobates* receptor that S108C with or without F106L had a significantly reduced maximal current (Fig. 3A, B). The observations in *Epipedobates* are particularly revealing as they show that adding the probable ancestral and highly conserved amino acid, serine, increases receptor currents compared with the *Epipedobates* wild-type that contains cysteine in that position. Thus, a major effect of the S108C substitution in the $\beta 2$ nAChR subunit is to decrease maximal currents compared with serine-containing $\beta 2$ subunits obtained with similar amounts of RNA. Such a decrease in macroscopic currents would potentially compromise synaptic transmission, with presumed downstream effects on organismal function.

S108C decreases the number of nAChRs in the plasma membrane

In principle, a decrease in current magnitude induced by the cysteine substitution could be due to (1) a reduction in the total number of functional receptors on the cell surface or (2) changes in the biophysical/kinetic properties of the expressed receptors. We tested the first alternative with *Epipedobates* $\alpha 4\beta 2$ nAChRs by measuring the number of receptors in the plasma membrane of intact

oocytes labeled with a radiolabeled antibody (^{125}I -mAb 295) that specifically binds to the $\beta 2$ nAChR subunit of mature $\alpha 4\beta 2$ nAChRs [32]. Additional file 1, in panels C–E, shows a fragment from monoclonal antibodies that similarly binds to the $\beta 2$ subunit of human $\alpha 4\beta 2$ nAChRs [33]. The iodinated antibody binds to chicken and mammalian receptors [34], and we now extend the species range by showing that it binds to frog receptors as well (Additional file 7, panels A and B). Additionally, the strong relationship ($R^2 = 0.83$) between maximum current and specific binding determined as described in the following paragraphs is further evidence that this antibody binds to frog nAChRs (Additional file 7, panel C).

We injected RNAs encoding single *Epipedobates* $\alpha 4$ and $\beta 2$ nAChR subunits into oocytes and allowed them to incubate for 7 days [32, 35]. We confirmed that oocytes incubated for 7 days generate the same relative maximal currents profiles as those incubated for 4 days (Fig. 3A, B). In general, the presence of C108 in the $\beta 2$ nAChR subunit resulted in decreased macroscopic currents compared with $\beta 2$ S108-containing nAChRs, independently of the presence of F or L in position 106 in the $\beta 2$ subunit. Additionally, when the $\beta 2$ subunit was the limiting factor (7 α :1 β ratio), the current was decreased compared with the 1 α :7 β ratio.

In a ratio favoring $\beta 2$ subunit incorporation ($1\alpha:7\beta$), the number of receptors per oocyte measured using ^{125}I -mAb 295 was similar except for the wild-type *Epipredobates* receptor [$\beta 2(\text{LC})$], which was significantly lower (Fig. 3C). However, when β subunit concentration was limiting ($7\alpha:1\beta$), the presence of serine in position 108 in conjunction with phenylalanine in position 106 [$\beta 2(\text{FS})$, that is, the ancestral residues present in human, *Xenopus* and *Nanorana* $\beta 2$ subunits] significantly increased the number of $\alpha 4\beta 2$ nAChRs in the plasma membrane (Fig. 3B, C). This supports the hypothesis that the presence of C108 reduces the total number of $\alpha 4\beta 2$ nAChRs in the plasma membrane. It also suggests that the presence of L106 together with C108 is detrimental to receptor availability, which was unexpected since F106L was previously shown to compensate for the alterations in the ACh CRC caused by S108C ($\text{FS}=\text{LC}\neq\text{FC}$) in mammalian receptors [13].

Concatenated human nAChRs confirm results from frogs

The most parsimonious explanation for our results with frog receptors is that the presence of C108 in $\beta 2$ subunits limits the number of functional $\alpha 4\beta 2$ nAChRs by, for example, decreasing the efficiency of receptor assembly, trafficking, or stability. Could such an effect also explain our previous data on human receptors? The S108C substitution in human $\beta 2$ subunits biases the receptor toward more LS sites, especially when $\beta 2$ subunits are scarce ($7\alpha:1\beta$). The presence of C108 could either (1) directly alter ACh sensitivity in a $2\alpha:3\beta$ stoichiometry or (2) induce a $3\alpha:2\beta$ stoichiometry in which LS sites result from the inclusion of a third $\alpha 4$ subunit instead of a $\beta 2$, due, for instance, to $\alpha 4$ subunits outcompeting $\beta 2$ subunits during receptor assembly.

The injection of RNA into cells results in a mixed population of receptors with different stoichiometries. Biasing the ratios of RNA (e.g., 7:1) as we have done, strongly favors one stoichiometry over others. However, this is still not a pure population of HS or LS nAChRs. This can be overcome by using concatenated constructs in which the number and order of $\alpha 4$ and $\beta 2$ subunits are identical in all receptors because they are genetically encoded, covalently linked $\alpha 4$ and $\beta 2$ nAChR subunits (see the “Methods” section). To test between these alternatives, we generated a series of concatenated human $\alpha 4\beta 2$ nAChR constructs with fixed $2\alpha:3\beta$ configurations, but with one, two, or all three $\beta 2$ subunits containing the S108C substitution. If S108C induces LS sites in receptors with a $2\alpha:3\beta$ stoichiometry, the concatenated receptors would produce a biphasic ACh CRC with no decrease of the current magnitude. If S108C produces a deficiency in the subunits’ ability to assemble into functional pentamers and/or traffic to the plasma membrane,

then a monophasic ACh CRC (HS-like) and a decrease in current magnitude would be observed for the concatenated receptors.

We found that the currents of concatenated $\alpha 4\beta 2$ nAChR were dramatically decreased with a single S108C-containing subunit, and no currents could be recorded when S108C was present in two or three subunits (Fig. 4A–C and Table 3). Importantly, the ACh CRCs generated from concatenated $\alpha 4\beta 2$ nAChRs harboring a single S108C had no LS component and showed the same sensitivity to ACh as the concatenated wild-type receptor (Fig. 4A, Table 3, and Additional file 4). This supports the contention that the LS sites observed in human $\alpha 4\beta 2$ nAChRs formed from free subunits (Additional file 2, panel A) derive from replacing a $\beta 2$ subunit with an $\alpha 4$. In other words, the S108C substitution does not affect ACh actions on the canonical binding site that is proximal to the substitution, but rather modifies the receptor stoichiometry, and that leads to a decrease in ACh sensitivity.

Finally, we performed another set of recordings (Fig. 4D), but this time, we measured both maximal ACh-induced currents and the number of $\alpha 4\beta 2$ nAChRs in the plasma membrane in the same oocytes. The maximal currents followed the same pattern previously found (Fig. 4D) and, in agreement with the electrophysiology, the total cell-surface expression fell with a single S108C-containing $\beta 2$ subunit and were vanishingly small with two or three S108C $\beta 2$ subunits incorporated into the functional pentamer (Fig. 4E). Also, in agreement with the data from frogs, the addition of the F106L substitution did not compensate for S108C, neither in the maximal currents (Fig. 4F) nor the total number of nAChRs present in the plasma membrane (Fig. 4G). The fact that S108C decreases current magnitude in frog and human concatenated $\alpha 4\beta 2$ nAChRs emphasizes the general detrimental nature of this substitution on vertebrate $\alpha 4\beta 2$ nAChRs.

Discussion

Two lineages of dendrobatid frogs, *Epipredobates* and *Ameerega*, sequester the nAChR agonist epibatidine for defense [36, 37]. A $\beta 2$ cysteine substitution that decreases the $\alpha 4\beta 2$ nAChR sensitivity to epibatidine appears to have evolved three times in parallel in different groups of dendrobatids. Even though one of these three (*Oophaga*) is not known to sequester epibatidine, it sequesters other nAChR agonists or antagonists. The serine at this site (108) is otherwise highly conserved in vertebrate $\beta 2$ subunits, suggesting that substitutions at this site are maladaptive. Our previous work showed that, while the S108C substitution protected human receptors against epibatidine, it perturbed their ACh sensitivity, a potential cost

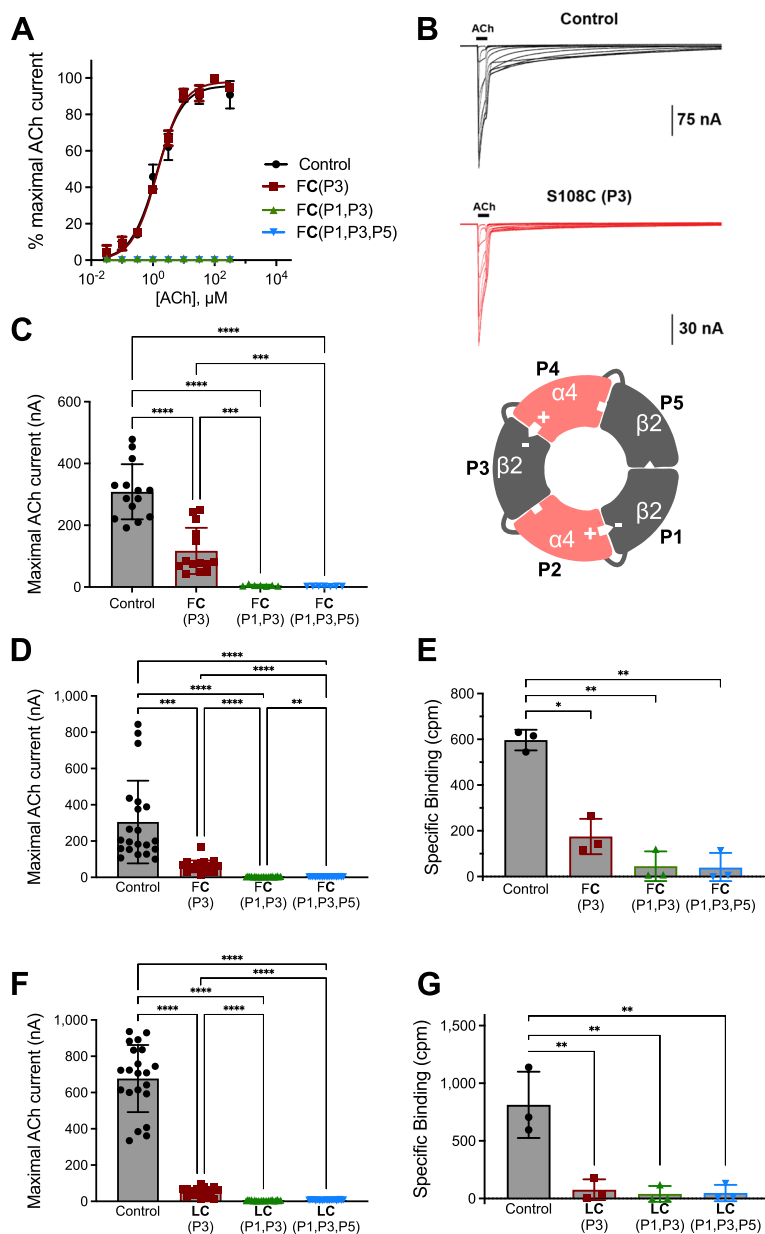


Fig. 4 Currents and number of receptors measured after the expression of concatenated human nAChRs. All concatemers have an enforced 2α:3β stoichiometry (indicated by the inset of the schematic receptor). **A** Wild-type receptor [F106 and S108, β2(FS), black] generates a CRC with a monophasic fit. A similar concentration–response profile was observed for concatenated α4β2 nAChRs with a S108C substitution (red, **FC**, substitution indicated by bold font; P3 = position 3 within the linked receptor) in a single β2 subunit. However, concatenated α4β2 nAChRs with two (green) or all three (blue) β2 subunits containing S108C in the indicated positions generate no current. CRC analysis can be found in Table 3 and Additional file 4, $n = 7–14$. **B** Raw current traces to increasing concentrations of ACh. **C** Concatemers where a single β2 subunit has a S108C substitution [β2(**FC**)] show significantly reduced currents. As stated in **A**, concatemers with two or three S108C-containing β2 subunits generate no current ($n = 7–14$). **D** We repeated the experiment shown in **C** and then measured the number of receptors in the plasma membrane in the same oocytes. Baseline recordings of maximal currents ($n = 21$). **E** Measurements of receptor number in the plasma membrane in oocytes from **D** ($n = 3$, 7 pooled oocytes in each experiment). **F** ACh-induced maximal currents in concatenated α4β2 nAChRs with an F106L substitution in addition to the S108C [β2(**LC**)] ($n = 21$). **G** Measurements of receptor number in the plasma membrane in oocytes from **F** ($n = 3$, 7 pooled oocytes in each experiment). The addition of F106L substitution to S108C [β2(**LC**)] did not rescue the effect of S108C. In both **E** and **G**, concatenated α4β2 nAChRs with a single S108C-containing β2 subunit have significantly reduced numbers of receptors in the plasma membrane when compared to controls. Those concatenated α4β2 nAChRs with two or three β2 subunits harboring the S108C mutation are not expressed in the plasma membrane (i.e., the values were no different from uninjected oocytes). Specific binding was measured as counts per minute (cpm). Data are shown as means ± SD and were analyzed using the Brown-Forsythe and Welch ANOVA tests, followed by Dunnett’s T3 multiple comparisons test. * $P < 0.05$, ** $P < 0.01$, *** $P < 0.001$, **** $P < 0.0001$

Table 3 Parameters from a non-linear curve fit of ACh concentration–response curves in oocytes expressing concatenated human $\alpha 4\beta 2$ nAChRs (2 $\alpha 4$:3 $\beta 2$)

Receptor	EC ₅₀ (μM)	n _H	I _{max} (%)	n
$\alpha 4\beta 2$ control	1.3 (1.2 to 1.5)	1.04 ± 0.05	96 ± 1	14
$\alpha 4\beta 2$ (FC) P3	1.4 (1.3 to 1.5)	1.06 ± 0.03	98 ± 1	14
$\alpha 4\beta 2$ (FC) P1, P3	–	–	0	7
$\alpha 4\beta 2$ (FC) P1, P3, P5	–	–	0	7

The data from each curve fit a single population (monophasic) curve. $\beta 2$ (FC) represents F106 and C108 in the $\beta 2$ subunit. The bold font indicates a substitution in the wild-type background. P1, P3, and P5 refer to the position of the $\beta 2$ subunit in the concatemer (Fig. 4)

Dashes signify no currents

EC₅₀ effective concentration 50 (concentration that produces 50% of maximal response), expressed as mean (95% confidence intervals); n_H Hill coefficient, expressed as mean ± SEM; I_{max} maximal current, expressed as a percentage of maximal response (mean ± SEM); n number of oocytes

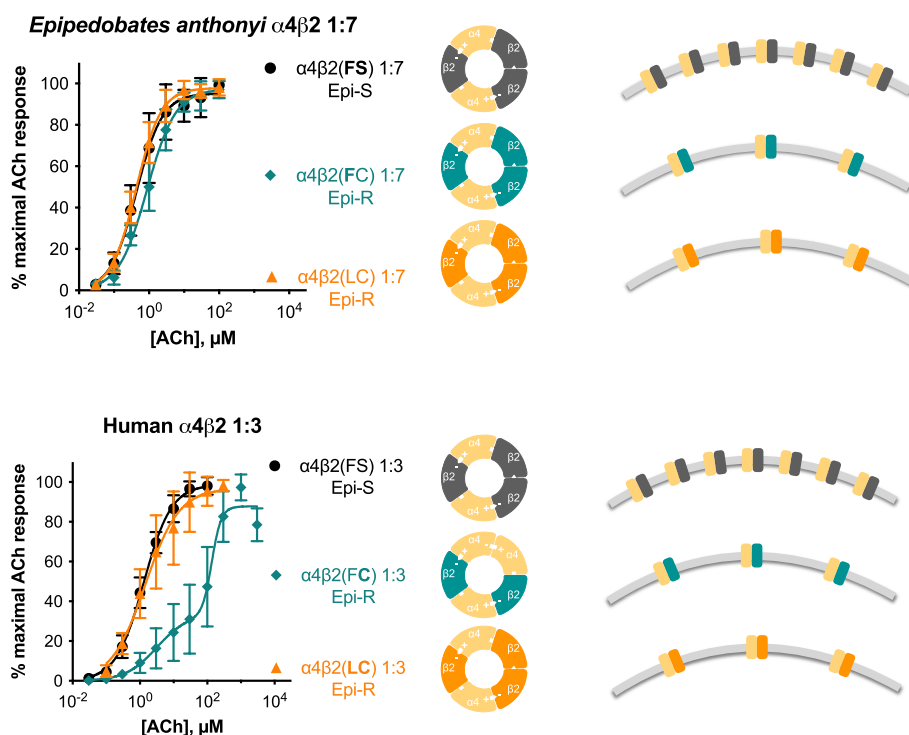


Fig. 5 Summary figure. Results from Tarvin et al. [13] are shown in the graphs on the left, from *Epipedobates anthonyi* (top, n = 5–9) and human (bottom, n = 6–7) nAChRs (RNA ratio 1 α :7 β for *Epipedobates* and 1 α :3 β for human). Epi-S and Epi-R refer to the epibatidine-sensitive and epibatidine-resistant characteristics of the receptor. These results led us to hypothesize that the mutation S108C in the human $\beta 2$ subunit [$\alpha 4\beta 2$ (FC)] resulted in an altered stoichiometry: instead of a monophasic curve (characteristic of $\alpha 4\beta 2$ nAChRs composed of 2 $\alpha 4$ and 3 $\beta 2$ subunits), the ACh concentration–response curve for this mutant was biphasic and shifted to the right (characteristic of $\alpha 4\beta 2$ nAChRs composed of 3 $\alpha 4$ and 2 $\beta 2$ subunits). Furthermore, this alteration in the ACh sensitivity was not observed in *Epipedobates* receptors, which showed the same monophasic curve at all RNA ratios tested (Additional file 2). In the central panels, the predicted stoichiometry is shown as a diagram of the receptor. We now report that there is a reduction of maximal ACh-induced currents in *Epipedobates* receptors with C108-containing $\beta 2$ subunits, likely due to reduced availability of C108-containing $\beta 2$ subunits (Fig. 3). The relative number of receptors in the plasma membrane is shown on the right diagrams. No differences in ACh sensitivity were observed after biasing $\alpha 4$ and $\beta 2$ RNA injection ratios, indicating that *Epipedobates* $\alpha 4\beta 2$ nAChRs functionally assemble in a single stoichiometry. However, the reduced cell-surface expression of $\alpha 4\beta 2$ (FC) nAChRs (also observed for *Epipedobates* $\alpha 4\beta 2$ nAChRs containing cysteine in position 108 of the $\beta 2$ subunit) alters the concentration–response profile of human $\alpha 4\beta 2$ (FC) receptors from the monophasic (HS-like) of the wild-type nAChR to biphasic (LS-like) CRC, indicating an alternative stoichiometry. The presence of an additional mutation [$\beta 2$ (LC)] confers an HS-like stoichiometry but does not correct the $\beta 2$ -reduced availability. The studies on the human receptor numbers in the plasma membrane were obtained using concatenated receptors (Fig. 4)

(Fig. 5). However, we also found that the S108C substitution had little to no effect on the ACh sensitivity of dendrobatid receptors, suggesting three possibilities: that this advantageous substitution is cost-free in frogs, that the cost manifests in other properties of nAChR function, or that there are additional, unrecognized dendrobatid-specific substitutions that prevent perturbation of ACh sensitivity [38].

We tested the “unknown dendrobatid-specific substitution” hypothesis by assessing concentration–response profiles of the endogenous neurotransmitter ACh of two phylogenetically divergent non-dendrobatid frogs, with the expectation that these species would show perturbations of ACh CRCs similar to those of human $\alpha 4\beta 2$ nAChRs. But the ACh sensitivity of these frog nAChRs were also unaffected by the S108C substitution.

Unexpectedly, however, in both dendrobatid and non-dendrobatid frogs, S108C induced a drastic reduction of ACh-activated maximal currents and the number of $\alpha 4\beta 2$ -containing nAChRs in the plasma membrane, exposing a potential detriment due to the S108C substitution. This is particularly notable in that introduction of the probable ancestral serine into *Epipedobates* $\beta 2$ subunit markedly rescues current levels and numbers of $\alpha 4\beta 2$ nAChRs in the plasma membrane over its wild-type cysteine-containing $\beta 2$ subunit. In sum, we now report that there is a reduction of maximal ACh-induced currents in *Epipedobates* receptors with C108-containing $\beta 2$ subunits, likely due to reduced availability of C108-containing $\beta 2$ subunits.

The F106L substitution has a minimal effect

Like S108, F106 is highly conserved in vertebrate $\beta 2$ subunits (Fig. 1). We previously observed that F106L wholly or partially rescued the effects of S108C on the CRCs of human $\alpha 4\beta 2$ nAChRs assembled from single nAChR subunits [38] although this substitution had no effect on ACh sensitivity in *Epipedobates*. In the present study, we saw little effect, or occasionally even a detrimental effect, of F106L on the current magnitude or receptor numbers with $\alpha 4\beta 2$ nAChRs expressed from free frog or concatenated human subunits. It is possible that the corrective effect of F106L in the ACh sensitivity of human $\alpha 4\beta 2$ (S108C) nAChRs is dependent on the subunits being free, so that the F106L substitution can modify the stoichiometry back to the $2\alpha:3\beta$ composition given the RNA ratio injected. This is not possible if the human subunits are concatenated or unable to form alternative stoichiometries, as is the case in frog receptors. One possibility is that F106L affects the biophysical properties of the receptors (e.g., single-channel open probability, open and/or closed dwell times) which we did not study here, to counteract the detrimental effects of S108C. Additionally, *Epipedobates anthonyi* apparently sequesters other alkaloids chemically similar to epibatidine such as N-methyl epibatidine and phantasmidine [39], and it is possible that F106L protects against those. At the moment, we are unable to assign any adaptive value to the F106L substitution in *Epipedobates* nAChRs.

Potential cost of S108C is decreased number of receptors in the plasma membrane

The most parsimonious explanation for our results is that S108C causes the $\beta 2$ subunit to be less efficient in its synthesis or folding, or in the assembly, trafficking, and/or stability of the functional pentamer. Indeed, the $\beta 2$ subunit limits the rate of receptor assembly [40, 41] and entry into the endoplasmic reticulum [42]. If S108C were to cause $\beta 2$ subunits to assemble poorly or assembled

pentamers to be trafficked less efficiently, S108C-containing subunits would produce fewer functional receptors than an equivalent number of $\beta 2$ subunits without this substitution. By the law of mass action, this would be especially evident when the number of $\beta 2$ subunits is low, as we have demonstrated in this study using expression ratios of $7\alpha:1\beta$.

This explanation also fits the effects of S108C on mammalian $\alpha 4\beta 2$ nAChRs. S108C in a mammalian $\beta 2$ subunit biases the receptor toward more LS receptors, most likely by modifying the stoichiometry of the receptor, not by changing the ACh actions in the canonical binding site proximal to the S108C substitution. A $\beta 2$ subunit that associates less efficiently would allow more $\alpha 4$ subunits to be incorporated into assembling receptors, modifying the stoichiometry into a LS receptor, resulting in a rightward shift of the ACh CRC that was evident in our previous work (Additional file 2, panels A and B).

Conclusions

While the S108C substitution may bestow epibatidine resistance on the $\alpha 4\beta 2$ nAChRs, the decrease in the numbers of receptors in the plasma membrane would be expected to incur a cost if the number of receptors became limiting, leading to decreased cholinergic synaptic transmission unless this is remedied by further adaptations. Recent evidence highlights the importance of chaperones (a protein that interacts with another protein to acquire its functionally active conformation), including nAChR-specific chaperones, in determining nAChR subunit stoichiometry and trafficking (movement of proteins within or out of the cell) in mammals [43–45]. Poison frogs might compensate for S108C-dependent assembly inefficiency by regulating receptor stoichiometry or availability via chaperones. Other possible solutions to this problem would be upregulation of genes or proteins for nAChR subunits or chaperones in the brain, which could be examined with transcriptomic and proteomic studies of dendrobatid brains. For example, a simple prediction from our results is that to compensate for reduced levels of $\alpha 4\beta 2$ nAChRs, dendrobatids with the $\beta 2$ S108C substitution must constantly generate extremely high levels of mRNA and/or protein for $\beta 2$ subunits compared with dendrobatids without S108C or non-dendrobatids, to ensure an abundant population of $\beta 2$ -containing receptors; this would levy a continuing metabolic cost.

Methods

Chemicals

All chemicals and solvents were of analytical grade, purchased from Sigma-Aldrich (St. Louis, MO) and Life Technologies (Grand Island, NY). The iodinated monoclonal antibody ^{125}I -mAb295 was kindly provided by Dr.

Jon Lindstrom (University of Pennsylvania; Philadelphia, PA) and Dr. Paul Whiteaker (The Barrow Neurological Institute, Phoenix, AZ).

In vitro transcription of single subunits

For experiments with single (non-concatenated) subunits, we used DNA encoding $\alpha 4$ and $\beta 2$ nAChR subunits (chrna4 and chrnb2) from different species. DNA encoding *Xenopus* subunits cloned in pCMV-SPORT6 were obtained from Dharmacon (Lafayette, CO). DNAs encoding *Epipedobates* and *Nanorana* nAChR subunits were optimized for expression in *Xenopus laevis* oocytes, synthesized de novo, and subcloned in pGEMHE by GenScript (Piscataway, NJ). Complementary DNAs encoding human nAChR subunits were cloned in pSP64. After linearizing the plasmids, nAChR subunits were in vitro transcribed using mMessage mMachine (Life Technologies, Grand Island, NY). RNA concentration and quality were checked using a ND-1000 spectrophotometer (NanoDrop Technologies, Wilmington, DE), electrophoresis (either Bioanalyzer or TapeStation systems, Agilent, Santa Clara, CA), or fluorometry (Qubit, Thermo Fisher Scientific, Waltham, MA). RNA stocks were stored at $-80\text{ }^{\circ}\text{C}$ and aliquots were stored at $-20\text{ }^{\circ}\text{C}$.

Oocyte isolation and injection of single subunits

Mature *Xenopus laevis* frogs were obtained from Nasco (Fort Atkinson, WI) and housed in the University of Texas animal facility. Frogs underwent partial oophorectomy under tricaine anesthesia, and the piece of the ovary was placed in isolation media (108 mM NaCl, 2 mM KCl, 1 mM EDTA, 10 mM HEPES, pH=7.5). Using forceps, the thecal and epithelial layers were manually removed from stage V and VI oocytes. Isolated oocytes were treated with collagenase from *Clostridium histolyticum* (83 mM NaCl, 2 mM KCl, 1 mM MgCl₂, 5 mM HEPES, and 0.5 mg mL⁻¹ collagenase) for 10 min to remove the follicular layer. Each oocyte was injected into the cytoplasm using a microinjector (Drummond Scientific Company, Broomall, PA) with RNA encoding nAChR single subunits in a volume of 50 nL. The subunits were either wild-type or with substitutions in either position 106 and or 108 of the $\beta 2$ subunit (numeration corresponds to the mature protein). For *Xenopus* subunits, 1 $\alpha 4$:3 $\beta 2$ W/W ratio: 6 ng total RNA for FS (F106, S108; wild-type) receptors and 20 ng total RNA for FC and LC mutants (the residue in bold font is the substitution); 7 $\alpha 4$:1 $\beta 2$ W/W ratio: 23 ng total RNA for FS receptors and 32 ng total RNA for FC and LC receptors. For *Nanorana* subunits, 1 $\alpha 4$:3 $\beta 2$ W/W ratio: 10 ng total RNA for all genotypes; 7 $\alpha 4$:1 $\beta 2$ W/W ratio: 24 ng total RNA for all genotypes. For *Epipedobates* subunits, 16 ng total RNA for all genotypes and all ratios ($\alpha 4$: $\beta 2$ in 1:7 or 7:1

W/W). For human subunits, 10 ng total RNA for all genotypes and all ratios ($\alpha 4$: $\beta 2$ in 1:3 or 3:1 W/W). For *Xenopus* and *Nanorana*, we aimed to maximize the current and injected variable amounts of RNA depending on the construct and α : β ratio. Oocytes were then incubated at 16 °C in sterile incubation solution (88 mM NaCl, 1 mM KCl, 2.4 mM NaHCO₃, 19 mM HEPES, 0.82 mM MgSO₄, 0.33 mM Ca(NO₃)₂, 0.91 mM CaCl₂, 10,000 units/L penicillin, 50 mg/L gentamicin, 90 mg/L theophylline, and 220 mg/L sodium pyruvate, pH=7.5). Incubation periods varied from 3 to 5 days.

Electrophysiological recordings of single subunits

Responses to acetylcholine (ACh) were studied 3–5 days after injection through two-electrode voltage clamp (Oocyte Clamp OC-725C, Warner Instruments, Hamden, CT) and digitized using a PowerLab 4/30 system (ADInstruments, Colorado Springs, CO). The oocytes were placed in a rectangular chamber and continuously perfused at a rate of 2 mL min⁻¹ with Ba-ND96 + Atropine buffer (96 mM NaCl, 2 mM KCl, 1 mM BaCl₂, 1 mM MgCl₂, 10 mM HEPES, 1 μ M atropine) at room temperature. Oocytes were clamped at -70 mV using two glass electrodes filled with 3 M KCl. All drugs were applied by bath perfusion, and solutions were prepared on the day of the application.

Concentration–response curves (CRCs) for ACh were obtained by applying increasing concentrations (20–30 s applications) with 5–15 min washout times. All responses were normalized to the maximal ACh response seen in that oocyte by assigning it a 100% value. Maximal current values (I_{max}) were obtained from the CRCs or from applying a single ACh concentration determined to produce maximal current based on previous CRCs [13].

Preparation of high-sensitivity, concatenated $\alpha 4\beta 2$ -nAChR DNA constructs containing human or mutant $\beta 2$ -nAChR subunits

The engineering and design of human $\alpha 4\beta 2$ -nAChRs adhered to methods previously described for concatenated nAChR DNA constructs [32, 46]. Briefly, all but the first $\beta 2$ subunit were absent their start codons and signal peptides, and all but the last were devoid of a stop codon. Each nAChR subunit was linked to its neighbor by a short stretch of nucleotides encoding a series of 6 or 9 (Ala-Gly-Ser)_n repeats, engineered to ensure a total linker length (including the C-terminal tail of the preceding subunit) of 40 ± 2 amino acids. GeneArt custom gene synthesis (Invitrogen; Waltham, MA) was used to design, synthesize, and sequence-verify optimized human (FS; control) and mutant $\beta 2$ nAChR subunits (either F106L, S108C, or both). A unique set of six restriction sites either flanking the entire concatemer or approximately

bisecting each linker between subunits was introduced along the concatenated sequence [32]. This permitted the replacement of individual subunits using standard restriction digestion and ligation methods. As previously demonstrated, the initial $\beta 2$ - $\alpha 4$ subunit pair of the $\alpha 4\beta 2$ -nAChR will assemble to form an orthosteric binding site between the complementary (–) face of the initial $\beta 2$ subunit and the principal (+) face of the following $\alpha 4$ subunit [32, 47]. Each $\alpha 4\beta 2$ -nAChR construct was subcloned into the pSGEM oocyte high expression vector and assembly of each construct was verified by restriction digest. Subunits for $\alpha 4\beta 2$ -nAChRs were designed in the order $\beta 2$ - $\alpha 4$ - $\beta 2$ - $\alpha 4$ - $\beta 2$ for the human $\alpha 4\beta 2$ -nAChR construct (control). Accordingly, the assembled plesiomorphic human $\alpha 4\beta 2$ -nAChR genotype hosts orthosteric agonist binding pockets at the $\alpha 4(+)/(-)\beta 2$ interfaces between the first and second and the third and fourth subunits [47].

To investigate the contributions of poison frog amino acid substitutions in human genetic background, concatenated human $\alpha 4\beta 2$ -nAChR constructs were engineered with single mutant $\beta 2$ -nAChR subunit genotypes containing the amino acid patterns FC (i.e., substitution S108C) and LC (i.e., double substitution F106L,S108C), as identified in *Epipedobates* [13]. Initially, human $\alpha 4\beta 2$ -nAChR construct sequences were expressed with the mutant FC (i.e., S108C), a sequence known to confer epibatidine resistance in frogs [13]. Human $\alpha 4\beta 2$ -nAChR constructs were engineered with this amino acid substitution using the following stoichiometries: $\beta 2(\text{FC})$ - $\alpha 4$ - $\beta 2$ - $\alpha 4$ - $\beta 2$, $\beta 2(\text{FC})$ - $\alpha 4$ - $\beta 2(\text{FC})$ - $\alpha 4$ - $\beta 2$, and $\beta 2(\text{FC})$ - $\alpha 4$ - $\beta 2(\text{FC})$ - $\alpha 4$ - $\beta 2(\text{FC})$. Additional human $\alpha 4\beta 2$ -nAChR constructs were engineered to express the double substitution within the $\beta 2$ -nAChR subunit at three different positions: $\beta 2(\text{LC})$ - $\alpha 4$ - $\beta 2$ - $\alpha 4$ - $\beta 2$, $\beta 2(\text{LC})$ - $\alpha 4$ - $\beta 2(\text{LC})$ - $\alpha 4$ - $\beta 2$, and $\beta 2(\text{LC})$ - $\alpha 4$ - $\beta 2(\text{LC})$ - $\alpha 4$ - $\beta 2(\text{LC})$.

Concatemer RNA preparation for oocyte injection

All concatenated $\alpha 4\beta 2$ -nAChR DNA plasmids were linearized with *Swa*I (2 h at 37 °C), treated with proteinase K (30 min at 50 °C), and purified using Qiagen's PCR Clean-up Kit (Valencia, CA); cRNAs were transcribed using the mMessage mMachine T7 kit (Applied Biosystems/Ambion, Austin, TX) and were purified using the Qiagen RNeasy Clean-up kit and stored at – 80 °C. RNA length and quality were confirmed on a 1% agarose gel.

Oocyte preparation and injection of RNA encoding human concatenated subunits

For expression of the human concatenated nAChRs, *Xenopus laevis* oocytes were isolated and processed for receptor expression as described in accordance with Lucero et al. [32] and with the following modification(s): *X.*

laevis oocytes were purchased from Ecocyte LLC (Austin, TX), maintained at 16 °C and injected with 80 nL containing 20 ng of RNA.

Two-electrode voltage clamp (TEVC) recordings of human concatenated $\alpha 4\beta 2$ -nAChRs

Detailed methodology for obtaining ACh CRCs and I_{max} from human concatenated nAChR-injected oocytes can be found in [32, 35]. Briefly, 7 days post-injection (for maximal expression of concatenated DNA constructs) oocytes were voltage clamped at – 70 mV with an Axoclamp 900A amplifier (Molecular Devices, Sunnyvale, CA). Recordings were sampled at 10 kHz (low pass Bessel filter, 40 Hz; high pass filter, direct current), and the traces were extracted and analyzed using the Clampfit software (Molecular Devices). Oocytes with leak currents > 50 nA were discarded and not used for analysis. Drugs were applied at a flow rate of 4 mL min^{–1} using a 16-channel, gravity-fed perfusion system with automated valve control (AutoMate Scientific, Inc., Berkeley, CA). Oocytes were recorded in OR2 buffer (82.5 mM NaCl, 2.5 mM KCl, 1 mM MgCl₂, 5 mM HEPES, pH 7.6; 22 °C) supplemented with atropine sulfate (1.5 μ M) to block endogenous muscarinic responses. ACh was acutely perfused for 1 s with a 60-s washout between ACh applications. All CRC recording sessions included oocytes injected mutant and wild-type controls (seven oocytes per group) to account for day-to-day and batch-to-batch variability in functional expression levels.

¹²⁵I-mAb 295 cell-surface labeling of $\alpha 4\beta 2$ -nAChRs

Surface expression levels of *Epipedobates* and human concatenated $\alpha 4\beta 2$ -nAChRs were quantified with ¹²⁵I-mAb 295 in an oocyte binding assay. For consistency, wild-type and mutant $\alpha 4\beta 2$ -nAChRs were tested on the same day. The iodinated monoclonal antibody, ¹²⁵I-mAb 295, specifically recognizes correctly folded human, bovine, and rodent $\beta 2$ -nAChR subunits [34, 48, 49] and immunolabeling protocols using this antibody have previously been described [21, 50]. We determined ¹²⁵I-mAb 295 specificity to frog $\alpha 4\beta 2$ -nAChR isoforms by comparing the specific binding of oocytes expressing *Epipedobates* $\alpha 4\beta 2$ -nAChR channels against uninjected oocytes (nonspecific controls; see below). Oocytes were injected with $\alpha 4\beta 2$ unbiased RNA ratios. Following injection, oocytes were incubated for 7 days prior to measuring cell-surface expression (see below). Oocytes expressing *Epipedobates* $\alpha 4\beta 2$ -nAChRs showed significantly higher levels of cell-surface binding compared to uninjected oocytes (Additional file 4), demonstrating that ¹²⁵I-mAb295 recognizes *Epipedobates* $\beta 2$ -nAChR subunit when heterologously expressed in *Xenopus* oocytes.

For immunolabeling experiments with *Epipedobates* $\alpha 4\beta 2$ -nAChRs, oocytes were isolated, decollagenased, and injected as described above for single subunits. Half of the oocytes were maintained at 16 °C in Austin for maximal current experiments conducted on day 4 after injection for comparison with other frog channels (peak current elicited with a maximal concentration of ACh, 100 μ M, 20 s, 2 mL min⁻¹). The other half were shipped overnight to the Barrow Neurological Institute (Phoenix, AZ) to measure the amount of $\alpha 4\beta 2$ -nAChR cell-surface expression and conduct maximal current experiments (concentration: 1 mM ACh, application duration: 1 s, flow rate: 4 mL min⁻¹), both on day 7 after injection. Oocytes were shipped in vials of incubation solution packed in a styrofoam box with a cold pack to keep the oocytes cool and then stored at 16 °C upon arrival. Despite the travel and slight variations in methodology, the observed pattern of I_{\max} remained consistent.

After I_{\max} experiments on day 7, oocytes were sorted into sets of seven (each expressing wild type or mutant concatenated $\alpha 4\beta 2$ -nAChR isoforms) on a 24-well plate (one set per well). The accompanying OR2 buffer was aspirated from each well and replaced with 2 nM ¹²⁵I-mAb 295 in OR2, supplemented with 10% heat-inactivated fetal bovine serum (to reduce nonspecific binding) and incubated with gentle agitation for 3 h at 22 °C. Washes were performed by aspiration of the radiolabeled solution and replacement with ice-cold OR2 supplemented with 10% heat-inactivated fetal bovine serum (2 mL well⁻¹). The oocytes were then transferred to a fresh 24-well plate with the minimum possible volume of diluted radioactive solution. This wash protocol was repeated three times before transferring the oocytes to a fresh 24-well plate. Oocytes were then lysed overnight in 0.1% SDS, 0.01 N NaOH (0.5 mL), prior to scintillation counting at 85% efficiency using a Packard TriCarb 1900 Liquid Scintillation Analyzer (PerkinElmer Life Sciences; Waltham, MA). One or more wells of non-injected oocyte controls were included per assay plate to determine nonspecific binding. Nonspecific binding was subtracted from the total binding determined in each of the other wells of the same plate to calculate specific binding. Surface expression for human concatenated mutant channels were determined similarly, modified with preparation as described for concatenated channels and no tests of I_{\max} on day 4.

Statistical analysis

The results were expressed as mean \pm SD, unless otherwise indicated. All statistical analysis was performed with Prism 8 (GraphPad Software Inc., San Diego, CA). For CRCs, the mean percent of maximal current for each

concentration was plotted and fitted to monophasic (Eq. 1) or biphasic (Eq. 2) logistic equations. The best-fitted equation was determined by applying the extra sum-of-squares *F* test. The corresponding *F*(DFn,DFd) values corresponding to each comparison are listed in Additional 4; a significance level of *p* < 0.01 was used so that the analysis could properly differentiate between the two models. Once the correct equation was identified, all parameters (log EC₅₀, Hill coefficients, and maximal currents) were determined. All relevant CRC parameters are shown in Tables 1, 2, and 3, and Additional file 4.

$$I = \frac{\text{Maximal current}}{1 + 10^{(\log EC_{50} - \log[\text{agonist}]) \times n_H}} \quad (1)$$

$$I = \frac{\text{Maximal current}_{HS}}{1 + 10^{(\log EC_{50,HS} - \log[\text{agonist}]) \times n_{H,HS}}} + \frac{\text{Maximal current}_{LS}}{1 + 10^{(\log EC_{50,LS} - \log[\text{agonist}]) \times n_{H,LS}}} \quad (2)$$

I, measured current; *Maximal current* achieved, expressed as a percentage of the maximal ACh response recorded in that oocyte; EC₅₀, effective concentration 50, or concentration that produces half the maximal current; *n_H*, Hill coefficient. In the case of biphasic curves (which reflect two kinds of binding sites), subscripts HS and LS were used to identify the two kinds of populations (HS, high sensitivity; LS, low sensitivity).

In the ¹²⁵I-mAb 295 immunolabeling experiments, total cell-surface binding was determined for each individual experiment (seven pooled oocytes/experimental group/experimental day) then averaged across three experimental days. For each experiment, uninjected oocytes were used to calculate non-specific binding. Specific counts were determined by subtracting the average non-specific counts from the average total binding [32, 35].

Maximal currents and specific binding were analyzed using one or two-way analysis of variance (ANOVA), followed by pairwise comparisons corrected for multiple comparisons as indicated in the legend. A significance level of *p* < 0.05 was used for these analyses.

Abbreviations

ACh	Acetylcholine
β2(FC)	Phenylalanine in position 106 and cysteine in position 108 in the β2 subunit
β2(FS)	Phenylalanine in position 106 and serine in position 108 in the β2 subunit
β2(LC)	Leucine in position 106 and cysteine in position 108 in the β2 subunit
β2(LS)	Leucine in position 106 and serine in position 108 in the β2 subunit
HS	High sensitivity
LS	Low sensitivity
nAChR	Nicotinic acetylcholine receptor

Supplementary Information

The online version contains supplementary material available at <https://doi.org/10.1186/s12915-023-01637-8>.

Additional file 1. Subunit arrangements and structure of $\alpha 4\beta 2$ nAChRs in different stoichiometries. (A and B). Diagrams of nAChRs in different stoichiometries, seen from the extracellular side. (A) nAChR formed by two $\alpha 4$ and three $\beta 2$ subunits ($2\alpha:3\beta$) that possesses high sensitivity (HS) binding sites for ACh located at $\alpha 4(+); \beta 2(-)$ interfaces. (B) nAChR formed by three $\alpha 4$ and two $\beta 2$ subunits ($3\alpha:2\beta$). In addition to the HS binding sites, it possesses a low sensitivity (LS) binding site for ACh located at the interface between two adjacent α subunits, $\alpha(+):\alpha(-)$. + and - signs indicate the principal and complementary components of the subunit interfaces. (C-E). Structure of human $\alpha 4\beta 2$ nAChRs determined by cryo-electron microscopy [33] with bound ligand and antibody fragments. (C) Stoichiometry $2:3\beta$ (Protein Data Bank, PDB: 6CNJ), viewed from the extracellular side. (D and E) Stoichiometry $3\alpha:2\beta$ (PDB: 6CNK), viewed from the membrane side (D) and the extracellular side (E). Molecular graphics performed with UCSF Chimera [51]. Alpha subunit in salmon, β subunit in grey, Fragment antigen-binding (Fab) from monoclonal antibodies in cyan. The arrows indicate the interfaces where nicotine (black, present in the structure) and acetylcholine bind. Red arrows indicate HS binding sites and blue arrows indicate LS binding site.

Additional file 2. Effects of reciprocal substitutions on ACh concentration-response curves (CRC) in the $\beta 2$ subunit of human and dendrobatid frog, *Epipedobates anthonyi*. Data redrawn from Tarvin et al. [13], presented as mean \pm SD. (A) A high ratio of $\beta 2$ to $\alpha 4$ ($1\alpha:3\beta$) of cRNA of the wild type human receptor subunits produces a monophasic CRC with a single EC_{50} indicating only high sensitivity (HS) binding sites (black curve: $\beta 2(\text{FS})$ represents F106 and S108 in $\beta 2$ subunit; $n = 7$). Introduction of the S108C substitution adds a low sensitivity (LS) binding site so that the CRC is now best fit with a biphasic curve reflecting both HS and LS sites (green curve: $\beta 2(\text{FC})$, amino acid in bold indicates a substitution; $n = 6$). Further addition of F106L to S108C eliminates the LS sites, thus compensating for the effect of S108C [orange curve: $\beta 2(\text{LC})$; $n = 6$]. (B) A low ratio of $\beta 2$ to $\alpha 4$ ($3\alpha:1\beta$) of the wild type human receptor subunits produces an ACh CRC shifted rightward and best fit with a monophasic curve with a shallow slope [black curve: $\beta 2(\text{FS})$; $n = 13$]. Introduction of the S108C substitution shifted the curve further right (green curve: $\beta 2(\text{FC})$; $n = 6$). Addition of F106L to S108C partially compensates for the effect of S108C alone [orange curve: $\beta 2(\text{LC})$; $n = 5$]. (C) When the ratio of injected human β subunit cRNA/ α subunit cRNA is high, the nAChR stoichiometry is $2\alpha:3\beta$. However, with paucity of β subunits the stoichiometry shifts to $3\alpha:2\beta$. (D,E) Even with more extreme ratios of α and β subunits (1:7 and 7:1) and the introduction of the ancestral amino acids (**FS**, **FC**), there was no change in the CRC of *Epipedobates anthonyi* ($n = 5-13$). (F) The stoichiometry of frog nAChR receptors is unknown but we conjectured it is $2\alpha:3\beta$ because they show a single kind of binding site (HS). This conjecture is noted by the question mark over the grey arrow.

Additional file 3. Accession numbers and names of species included in Fig. 1. The names of undefended species of poison frogs (Dendrobatidae) are in black and those of defended species are in blue.

Additional file 4. F(DFn, DFd) and p values from one- and two population fittings to ACh concentration-response curves, calculated using the Extra sum-of-squares F test. A value of $P < 0.10$ means the preferred model is the "Two populations" (biphasic curve); $P > 0.10$ means the preferred model is the "One population" (monophasic curve). DFn, degree of freedom for the numerator of the F ratio, DFd is for the denominator. The amino acids between parentheses stand for the residues at locations 106 and 108, respectively; if there is a substitution, the letter is in bold font.

Additional file 5. Representative tracings from ACh CRC from $\alpha 4\beta 2$ nAChR of two species of non-dendrobatids Tracings from *Xenopus tropicalis* $\alpha 4\beta 2$ nAChR with an $\alpha:\beta$ ratio of (A) 1:3 and (B) 7:1, and from *Nanorana parkeri* $\alpha 4\beta 2$ nAChR with an $\alpha:\beta$ ratio of (C) 1:3 and (D) 7:1. ACh concentration is indicated above each peak, in μM .

Additional file 6. Maximal currents from $\alpha 4\beta 2$ nAChR of two species of non-dendrobatids (A) *Xenopus tropicalis* ($n = 10-39$) (B) *Nanorana parkeri* ($n = 9-20$). The number over each bar indicates the total amount of cRNA (ng) injected per oocyte, while maintaining the $\alpha:\beta$ RNA ratio indicated. $\beta 2(\text{FS})$ represents F106 and S108 in the $\beta 2$ subunit. $\beta 2(\text{FC})$ and $\beta 2(\text{LC})$ indicates the residues present in position 106 and 108 in the $\beta 2$ subunit, with the bold font indicating substitutions in the wild type background. The different amounts of cRNA injected precluded a complete statistical analysis of each data set, but we performed a two-way ANOVA on the *Nanorana parkeri* data set, followed by a Holm-Sidak analysis to correct for multiple comparisons (all conditions against all conditions). We only show the significant differences within each RNA ratio, as those oocytes were injected with the same total amount of cRNA. ** $p < 0.01$, **** $p < 0.0001$.

Additional file 7. Antibody verification. Oocytes were injected with cRNA encoding *Epipedobates anthonyi* $\alpha 4\beta 2$ nAChRs (ratio 1:1, 4 ng each). (A) Currents induced by 1 mM ACh 7 days after injection ($n = 21$); uninjected oocytes were assumed to have no response to ACh based on previous experiments. (B) Raw counts obtained with an iodinated antibody directed against the $\beta 2$ subunit (^{125}I -mAb 295) in each group ($n = 3$ experiments with 7 pooled oocytes per experiment). (C) Correlation between the maximal ACh-induced current and the specific binding observed for each of the pooled oocytes expressing *Epipedobates* nAChRs tested for this study ($R^2 = 0.83$). $\beta 2(\text{LC})$ represents L106 and C108 in the $\beta 2$ subunit. When used for residues, the bold font indicates substitutions in the wild type background. Uninjected oocytes were used as blanks, and their counts subtracted from the values of injected oocytes for each experiment.

Acknowledgements

We thank Drs. Jon Lindstrom for his generous gift of iodinated antibody, John Mihic for the use of his lab space and equipment, and Sonia Mason and Jelena Todorovic for the experimental assistance.

Authors' contributions

Conceptualization: H.H.Z., D.C.C., J.M.Y., C.M.B., and A.A.G. Project administration: H.H.Z. Investigation: J.M.Y. and A.A.G. Formal analysis: J.M.Y., C.M.B., and A.A.G. Visualization: C.M.B., A.A.G., and D.C.C. Writing—original draft preparation: H.H.Z., C.M.B., A.A.G., and J.M.Y. Writing—review and editing: H.H.Z., D.C.C., A.A.G., C.M.B., and J.M.Y. Funding acquisition: H.H.Z., D.C.C., A.A.G., and J.M.Y. All authors read and approved the final manuscript.

Funding

This work was supported by NSF grant 1556967 (D.C.C. and H.H.Z.), National Institutes of Health R21 AG067029 (A.A.G.), and a Stengl-Wyer Graduate Fellowship from the University of Texas (J.M.Y.).

Availability of data and materials

All data generated or analyzed during this study are included in this published article and its supplementary information files. The datasets used and/or analyzed during the current study are available from the corresponding author upon reasonable request.

Declarations

Ethics approval and consent to participate

Frog care and surgery were conducted under IACUC-approved protocols (AUP-2015-00205 and AUP-2016-00016).

Consent for publication

Not applicable.

Competing interests

The authors declare that they have no competing interests.

Author details

¹Department of Neuroscience, The University of Texas, Austin, TX, USA.

²Department of Integrative Biology, and Biodiversity Center, The University

of Texas, Austin, TX, USA. ³Department of Neurobiology, The Barrow Neurological Institute, Phoenix, AZ, USA. ⁴Department of Pharmacology and Toxicology, Virginia Commonwealth University, Richmond, VA, USA.

Received: 6 October 2022 Accepted: 30 May 2023

Published online: 28 June 2023

References

- Geffeney SL, Fujimoto E, Brodie ED 3rd, Brodie ED Jr, Ruben PC. Evolutionary diversification of TTX-resistant sodium channels in a predator-prey interaction. *Nature*. 2005;434(7034):759–63.
- Petschenka G, Fandrich S, Sander N, Wagschal V, Boppre M, Dobler S. Stepwise evolution of resistance to toxic cardenolides via genetic substitutions in the Na⁺/K⁺-ATPase of milkweed butterflies (Lepidoptera: Danaini). *Evolution*. 2013;67(9):2753–61.
- Jost MC, Hillis DM, Lu Y, Kyle JW, Fozzard HA, Zakon HH. Toxin-resistant sodium channels: parallel adaptive evolution across a complete gene family. *Mol Biol Evol*. 2008;25(6):1016–24.
- Dalla S, Baum M, Dobler S. Substitutions in the cardenolide binding site and interaction of subunits affect kinetics besides cardenolide sensitivity of insect Na K-ATPase. *Insect Biochem Mol Biol*. 2017;89:43–50.
- Lee CH, Jones DK, Ahern C, Sarhan MF, Ruben PC. Biophysical costs associated with tetrodotoxin resistance in the sodium channel pore of the garter snake, *Thamnophis sirtalis*. *J Comp Physiol A Neuroethol Sens Neural Behav Physiol*. 2011;197(1):33–43.
- Ujvari B, Casewell NR, Sunagar K, Arbuckle K, Wuster W, Lo N, et al. Widespread convergence in toxin resistance by predictable molecular evolution. *Proc Natl Acad Sci U S A*. 2015;112(38):11911–6.
- Brodie ED 3rd, Brodie ED Jr. Costs of exploiting poisonous prey: evolutionary trade-offs in a predator-prey arms race. *Evolution*. 1999;53(2):626–31.
- McGugan JR, Byrd GD, Roland AB, Caty SN, Kabir N, Tapia EE, et al. Ant and mite diversity drives toxin variation in the little devil poison frog. *J Chem Ecol*. 2016;42(6):537–51.
- Neuwirth M, Daly JW, Myers CW, Tice LW. Morphology of the granular secretory glands in skin of poison-dart frogs (Dendrobatidae). *Tissue Cell*. 1979;11(4):755–71.
- Santos JC, Coloma LA, Cannatella DC. Multiple, recurring origins of aposematism and diet specialization in poison frogs. *Proc Natl Acad Sci U S A*. 2003;100(22):12792–7.
- Lopez JM, Smeets WJ, Gonzalez A. Choline acetyltransferase immunoreactivity in the developing brain of *Xenopus laevis*. *J Comp Neurol*. 2002;453(4):418–34.
- Yu CJ, Butt CM, Debski EA. Bidirectional modulation of visual plasticity by cholinergic receptor subtypes in the frog optic tectum. *Eur J Neurosci*. 2003;17(6):1253–65.
- Tarvin RD, Borghese CM, Sachs W, Santos JC, Lu Y, O'Connell LA, et al. Interacting amino acid replacements allow poison frogs to evolve epibatidine resistance. *Science*. 2017;357(6357):1261–6.
- Papke RL, Lindstrom JM. Nicotinic acetylcholine receptors: conventional and unconventional ligands and signaling. *Neuropharmacology*. 2020;168: 108021.
- Fu X, Moonschi FH, Fox-Loe AM, Snell AA, Hopkins DM, Avelar AJ, et al. Brain region specific single-molecule fluorescence imaging. *Anal Chem*. 2019;91(15):10125–31.
- Harpsoe K, Ahning PK, Christensen JK, Jensen ML, Peters D, Balle T. Unraveling the high- and low-sensitivity agonist responses of nicotinic acetylcholine receptors. *J Neurosci*. 2011;31(30):10759–66.
- Kouvatzos N, Giastas P, Chroni-Tzartou D, Pouloupoulou C, Tzartos SJ. Crystal structure of a human neuronal nAChR extracellular domain in pentameric assembly: ligand-bound alpha2 homopentamer. *Proc Natl Acad Sci U S A*. 2016;113(34):9635–40.
- Benallegue N, Mazzaferro S, Alcaïno C, Bermudez I. The additional ACh binding site at the alpha4(+)/alpha4(-) interface of the (alpha4beta2)2alpha4 nicotinic ACh receptor contributes to desensitization. *Br J Pharmacol*. 2013;170(2):304–16.
- Weltzin MM, George AA, Lukas RJ, Whiteaker P. Distinctive single-channel properties of alpha4beta2-nicotinic acetylcholine receptor isoforms. *PLoS ONE*. 2019;14(3): e0213143.
- Dash B, Bhakta M, Chang Y, Lukas RJ. Modulation of recombinant, alpha2*, alpha3* or alpha4*-nicotinic acetylcholine receptor (nAChR) function by nAChR beta3 subunits. *J Neurochem*. 2012;121(3):349–61.
- Kuryatov A, Lindstrom J. Expression of functional human alpha6beta2beta3* acetylcholine receptors in *Xenopus laevis* oocytes achieved through subunit chimeras and concatamers. *Mol Pharmacol*. 2011;79(1):126–40.
- Croxen R, Newland C, Beeson D, Oosterhuis H, Chauplannaz G, Vincent A, et al. Mutations in different functional domains of the human muscle acetylcholine receptor alpha subunit in patients with the slow-channel congenital myasthenic syndrome. *Hum Mol Genet*. 1997;6(5):767–74.
- McClure-Begley TD, Papke RL, Stone KL, Stokes C, Levy AD, Gelernter J, et al. Rare human nicotinic acetylcholine receptor alpha4 subunit (CHRNA4) variants affect expression and function of high-affinity nicotinic acetylcholine receptors. *J Pharmacol Exp Ther*. 2014;348(3):410–20.
- Matsumura N, Hirose S, Iwata H, Fukuma G, Yonetani M, Nagayama C, et al. Mutation (Ser284Leu) of neuronal nicotinic acetylcholine receptor alpha 4 subunit associated with frontal lobe epilepsy causes faster desensitization of the rat receptor expressed in oocytes. *Epilepsy Res*. 2002;48(3):181–6.
- Corrie LW, Stokes C, Wilkerson JL, Carroll FI, McMahon LR, Papke RL. Nicotinic acetylcholine receptor accessory subunits determine the activity profile of epibatidine derivatives. *Mol Pharmacol*. 2020;98(4):328–42.
- Fenster CP, Rains MF, Noerager B, Quick MW, Lester RAJ. Influence of subunit composition on desensitization of neuronal acetylcholine receptors at low concentrations of nicotine. *J Neurosci*. 1997;17(15):5747–59.
- Moroni M, Zwart R, Sher E, Cassels BK, Bermudez I. $\alpha\beta 2$ nicotinic receptors with high and low acetylcholine sensitivity: pharmacology, stoichiometry, and sensitivity to long-term exposure to nicotine. *Mol Pharmacol*. 2006;70(2):755–68.
- Zwart R, Vijverberg HP. Four pharmacologically distinct subtypes of alpha4beta2 nicotinic acetylcholine receptor expressed in *Xenopus laevis* oocytes. *Mol Pharmacol*. 1998;54(6):1124–31.
- Mazzaferro S, Bermudez I, Sine SM. $\alpha\beta 2$ nicotinic acetylcholine receptors: relationships between subunit stoichiometry and function at the single channel level. *J Biol Chem*. 2017;292(7):2729–40.
- Delsuc F, Philippe H, Tsigokogeorga G, Simion P, Tilak MK, Turon X, et al. A phylogenomic framework and timescale for comparative studies of tunicates. *BMC Biol*. 2018;16(1):39.
- Feng YJ, Blackburn DC, Liang D, Hillis DM, Wake DB, Cannatella DC, et al. Phylogenomics reveals rapid, simultaneous diversification of three major clades of Gondwanan frogs at the Cretaceous-Paleogene boundary. *Proc Natl Acad Sci U S A*. 2017;114(29):E5864–70.
- Lucero LM, Weltzin MM, Eaton JB, Cooper JF, Lindstrom JM, Lukas RJ, et al. Differential alpha4(+)/(-)beta2 agonist-binding site contributions to alpha4beta2 nicotinic acetylcholine receptor function within and between isoforms. *J Biol Chem*. 2016;291(5):2444–59.
- Walsh RM Jr, Roh SH, Gharpure A, Morales-Perez CL, Teng J, Hibbs RE. Structural principles of distinct assemblies of the human alpha4beta2 nicotinic receptor. *Nature*. 2018;557(7704):261–5.
- Whiting PJ, Lindstrom JM. Characterization of bovine and human neuronal nicotinic acetylcholine receptors using monoclonal antibodies. *J Neurosci*. 1988;8(9):3395–404.
- George AA, Bloy A, Miwa JM, Lindstrom JM, Lukas RJ, Whiteaker P. Isoform-specific mechanisms of alpha3beta4*-nicotinic acetylcholine receptor modulation by the prototoxin lynx1. *FASEB J*. 2017;31(4):1398–420.
- Aposematic poison frogs (Dendrobatidae) of the Andean countries: Bolivia, Colombia, Ecuador, Perú and Venezuela Kahn TR, La Marca E, Lötters S, Brown JL, Twomey E, Amézquita A, editors. Arlington: Conservation International; 2016. p. 588.
- Daly JW, Tokuyama T, Fujiwara T, Highet RJ, Karle IL. A new class of indolizidine alkaloids from the poison frog, *Dendrobates tricolor*. X-ray analysis of 8-hydroxy-8-methyl-6-(2'-methylhexylidene)-1-azabicyclo[4.3.0]nonane. *J Am Chem Soc*. 2002;124(2):830–6.
- Tarvin RD, Santos JC, O'Connell LA, Zakon HH, Cannatella DC. Convergent substitutions in a sodium channel suggest multiple origins of toxin resistance in poison frogs. *Mol Biol Evol*. 2016;33(4):1068–81.
- Fitch RW, Spande TF, Garraffo HM, Yeh HJ, Daly JW. Phantasmidine: an epibatidine congener from the Ecuadorian poison frog *Epipedobates anthonyi*. *J Nat Prod*. 2010;73(3):331–7.

40. Gu Y, Forsayeth JR, Verrall S, Yu XM, Hall ZW. Assembly of the mammalian muscle acetylcholine receptor in transfected COS cells. *J Cell Biol.* 1991;114(4):799–807.
41. Saedi MS, Conroy WG, Lindstrom J. Assembly of Torpedo acetylcholine receptors in *Xenopus* oocytes. *J Cell Biol.* 1991;112(5):1007–15.
42. Ren XQ, Cheng SB, Treuil MW, Mukherjee J, Rao J, Braunewell KH, et al. Structural determinants of $\alpha 4\beta 2$ nicotinic acetylcholine receptor trafficking. *J Neurosci.* 2005;25(28):6676–86.
43. Matta JA, Gu S, Davini WB, Lord B, Siuda ER, Harrington AW, et al. NACHO mediates nicotinic acetylcholine receptor function throughout the brain. *Cell Rep.* 2017;19(4):688–96.
44. Mazzaferro S, Whiteman ST, Alcaino C, Beyder A, Sine SM. NACHO and 14-3-3 promote expression of distinct subunit stoichiometries of the $\alpha 4\beta 2$ acetylcholine receptor. *Cell Mol Life Sci.* 2021;78(4):1565–75.
45. Srinivasan R, Henderson BJ, Lester HA, Richards CI. Pharmacological chaperoning of nAChRs: a therapeutic target for Parkinson's disease. *Pharmacol Res.* 2014;83:20–9.
46. Carbone AL, Moroni M, Groot-Kormelink PJ, Bermudez I. Pentameric concatenated $(\alpha 4)_2(\beta 2)_3$ and $(\alpha 4)_3(\beta 2)_2$ nicotinic acetylcholine receptors: subunit arrangement determines functional expression. *Br J Pharmacol.* 2009;156(6):970–81.
47. Zhou Y, Nelson ME, Kuryatov A, Choi C, Cooper J, Lindstrom J. Human $\alpha 4\beta 2$ acetylcholine receptors formed from linked subunits. *J Neurosci.* 2003;23(27):9004–15.
48. Lai A, Parameswaran N, Khwaja M, Whiteaker P, Lindstrom JM, Fan H, et al. Long-term nicotine treatment decreases striatal $\alpha 6^*$ nicotinic acetylcholine receptor sites and function in mice. *Mol Pharmacol.* 2005;67(5):1639–47.
49. Whiteaker P, Cooper JF, Salminen O, Marks MJ, McClure-Begley TD, Brown RW, et al. Immunolabeling demonstrates the interdependence of mouse brain $\alpha 4$ and $\beta 2$ nicotinic acetylcholine receptor subunit expression. *J Comp Neurol.* 2006;499(6):1016–38.
50. Eaton JB, Lucero LM, Stratton H, Chang Y, Cooper JF, Lindstrom JM, et al. The unique $\alpha 4+/-\alpha 4$ agonist binding site in $(\alpha 4)_3(\beta 2)_2$ subtype nicotinic acetylcholine receptors permits differential agonist desensitization pharmacology versus the $(\alpha 4)_2(\beta 2)_3$ subtype. *J Pharmacol Exp Ther.* 2014;348(1):46–58.
51. Pettersen EF, Goddard TD, Huang CC, Couch GS, Greenblatt DM, Meng EC, et al. UCSF Chimera—a visualization system for exploratory research and analysis. *J Comput Chem.* 2004;25(13):1605–12.

Publisher's Note

Springer Nature remains neutral with regard to jurisdictional claims in published maps and institutional affiliations.

Ready to submit your research? Choose BMC and benefit from:

- fast, convenient online submission
- thorough peer review by experienced researchers in your field
- rapid publication on acceptance
- support for research data, including large and complex data types
- gold Open Access which fosters wider collaboration and increased citations
- maximum visibility for your research: over 100M website views per year

At BMC, research is always in progress.

Learn more biomedcentral.com/submissions

